Cell

Ubiquitination Regulates PTEN Nuclear Import and Tumor Suppression

Lloyd C. Trotman,[1,2,11] Xinjiang Wang,[3] Andrea Alimonti,[1,2] Zhenbang Chen,[1,2] Julie Teruya-Feldstein,[2] Haijuan Yang,[4] Nikola P. Pavletich,[4,5] Brett S. Carver,[6] Carlos Cordon-Cardo,[2] Hediye Erdjument-Bromage,[7] Paul Tempst,[7] Sung-Gil Chi,[8] Hyo-Jong Kim,[9] Tom Misteli,[10] Xuejun Jiang,[3] and Pier Paolo Pandolfi[1,2,*]
[1] Cancer Biology and Genetics Program
[2] Department of Pathology
[3] Cell Biology Program
[4] Structural Biology Program
[5] Howard Hughes Medical Institute
[6] Department of Urology
[7] Molecular Biology Program
Sloan-Kettering Institute, Memorial Sloan-Kettering Cancer Center, New York, NY 10021, USA
[8] School of Life Sciences and Biotechnology, Korea University, Sungbuk-Gu, Seoul 136-701, Republic of Korea
[9] School of Medicine, Kyung Hee University, Seoul 130-701, Republic of Korea
[10] National Cancer Institute, National Institutes of Health, Bethesda, MD 20892, USA
[11] Present address: Cold Spring Harbor Laboratory, 1 Bungtown Road, Cold Spring Harbor, NY 11724, USA.
*Correspondence: p-pandolfi@ski.mskcc.org
DOI 10.1016/j.cell.2006.11.040

SUMMARY

The *PTEN* tumor suppressor is frequently affected in cancer cells, and inherited *PTEN* mutation causes cancer-susceptibility conditions such as Cowden syndrome. PTEN acts as a plasma-membrane lipid-phosphatase antagonizing the phosphoinositide 3-kinase/AKT cell survival pathway. However, PTEN is also found in cell nuclei, but mechanism, function, and relevance of nuclear localization remain unclear. We show that nuclear PTEN is essential for tumor suppression and that PTEN nuclear import is mediated by its monoubiquitination. A lysine mutant of PTEN, K289E associated with Cowden syndrome, retains catalytic activity but fails to accumulate in nuclei of patient tissue due to an import defect. We identify this and another lysine residue as major monoubiquitination sites essential for PTEN import. While nuclear PTEN is stable, polyubiquitination leads to its degradation in the cytoplasm. Thus, we identify cancer-associated mutations of PTEN that target its posttranslational modification and demonstrate how a discrete molecular mechanism dictates tumor progression by differentiating between degradation and protection of PTEN.

INTRODUCTION

Since the original identification of the tumor suppressor *p*hosphatase and *ten*sin homolog on chromosome TEN (*PTEN*) (Li et al., 1997; Steck et al., 1997), numerous reports have described *PTEN* loss or mutation in cancer specimens, cancer cell lines, and inherited cancer predisposing syndromes (Bonneau and Longy, 2000; Li et al., 1997), rendering this gene one of the most frequently affected tumor suppressors of the post-p53 era.

To better understand the causal nature of *PTEN* loss in human cancer, we and others have genetically modeled the effects of *Pten* loss in mice and have shown that such animals faithfully recapitulate the tumor spectrum observed in *PTEN*-deficient patients (Di Cristofano et al., 1998; Podsypanina et al., 1999; Suzuki et al., 1998; Trotman et al., 2003). These studies have firmly linked *Pten* loss to the stage of tumor initiation in epithelial cancer. Most notably, we have demonstrated *PTEN* haploinsufficiency (reviewed in Sherr [2004]), as a single copy becomes unable to prevent prostate cancer either in the context of loss of certain other tumor suppressor genes (Di Cristofano et al., 2001; Ma et al., 2005; Trotman et al., 2006) or, alternatively, in the context of genetically engineered reduction of *Pten* expression just below heterozygosity (Trotman et al., 2003). In addition, we have shown recently that complete *Pten* loss even provokes the p53-dependent cellular senescence response (Chen et al., 2005) that antagonizes prostate tumorigenesis, redefining the previously assumed interplay of these two major tumor suppressor genes (Trotman and Pandolfi, 2003). This finding further underscored the importance of a ''non-Knudsonian'' single-hit working model for loss of *PTEN* in tumor initiation and clarifies why indeed a majority of human tumors are retaining a wild-type (WT) copy of *PTEN* (Sansal and Sellers, 2004). Thus, understanding the mechanisms of PTEN regulation that govern this ''heterozygous tumor progression'' is imperative for progress in the field.

PTEN catalyzes the conversion of the membrane lipid second messenger PIP_3 to PIP_2 (Maehama and Dixon, 1998) and therefore is the key antagonist of various PIP_3-dependent proto-oncogenic kinases, chiefly among them AKT/PKB (Stambolic et al., 1998). This firmly links PTEN action to the cell's plasma membrane (Cantley, 2002; Di Cristofano and Pandolfi, 2000). However, it has long been observed that in several tissues and cultured cells PTEN is also found in cell nuclei (reviewed in Lian and Di Cristofano [2005]). While it remains unclear what function can be attributed to this nuclear pool of PTEN specifically, positive correlation between nuclear PTEN and suppression of tumor progression has been described for both cutaneous melanoma and colorectal cancer (Whiteman et al., 2002; Zhou et al., 2002). But in spite of such correlative studies, to date no proof for an essential role of nuclear PTEN in tumor suppression has been accrued. Furthermore, although these data suggested that nuclear PTEN could retain some activity, it still has remained unclear how PTEN subcellular localization would be regulated.

Nuclear protein import is generally mediated by distinct and, importantly, transferable nuclear localization signal (NLS) sequences such as the SV-40 T-antigen-like cluster of positively charged amino acids. Such sequences confer binding to import receptors, which mediate uni- or bidirectional transport across the nuclear pore complexes (NPCs; see Chook and Blobel [2001] and Gorlich and Kutay [1999]). Yet no functional NLS sequence satisfying the essential criteria has been found in PTEN, suggesting that PTEN either binds to another NLS-bearing protein to be transported in a "piggyback" fashion or that an altogether novel mechanism could regulate its nuclear import.

We describe here the discovery of a cancer-associated mutation that targets PTEN posttranslational modification and leads to an aberrant nuclear exclusion phenotype in a family of patients with Cowden syndrome (CS). CS is one of three closely related autosomal dominant cancer syndromes caused by germline-inactivating mutations of *PTEN* and is characterized by high cancer susceptibility (Eng, 2003). By identifying the biophysical, biochemical, and cell-biological deficiencies of this mutant, we here establish a causal relationship between PTEN posttranslational modification, nuclear import, and tumor initiation.

RESULTS

Nuclear Exclusion of $PTEN^{K289E}$ in Cowden Patient Polyps

We have previously solved the PTEN crystal structure (Lee et al., 1999), revealing an N-terminal phosphatase and a C-terminal C2 domain that stabilizes the catalytic domain and is essential for proper positioning of PTEN at the cell membrane (Georgescu et al., 2000 and see also Figure 1C). While most known PTEN missense mutations target the phosphatase domain, such as the catalytic cysteine 124 to arginine mutant (C124R, see abbreviations [Nelen et al., 1997]), some disrupt PTEN function by indirectly affecting catalytic domain architecture (Lee et al., 1999). Yet cancer-associated missense mutations have also been identified in regions of no apparent relevance to PTEN enzymatic function or stability. Prominent among them is a mutation found in a stretch of 32 amino acids within the C2 domain, which we term the C2 loop. This loop of PTEN is highly conserved among vertebrates, including zebrafish (Figure 1A). As previously described, the C2 loop (similar to N- and C-terminal tails of PTEN) interferes with proper crystal formation (Figure 1B) and can be specifically digested by subtilisin, consistent with a random and accessible conformation protruding from the framework of the C2 domain (Figure 1C). Importantly, C2 loop-deficient PTEN retains WT activity in vitro and in vivo (Lee et al., 1999). Yet, intriguingly, a missense mutation targeting a conserved residue of the C2 loop, K289E, has been described (see Figure 1A). In agreement with the above observations, $PTEN^{K289E}$ displays no significant defects in activity or membrane association (Georgescu et al., 2000), as K289 faces away from the plasma membrane (Figure 1C). Thus, taken together, the C2 loop has no positive structural function, its loss does not impinge on PTEN activity, and the C2 loop K289E mutant retains its enzymatic activity in vivo. Yet the K289E allele of *PTEN* is found inherited in a family in which carriers with one mutant allele display CS (Chi et al., 1998), thus demonstrating genetically that the K289E mutant is indeed defective in tumor suppression.

To investigate the paradox of how an enzymatically functional PTEN mutant can cause CS, we sought to study tumor samples of a family member who inherited the K289E mutation. Since these patients routinely undergo colonoscopy for removal of intestinal polyps, we analyzed this tissue (Figure 1D). Dysplastic intestinal polyps have large areas of poorly differentiated glandular structures at their surface (red rectangle, top), and this polyp's stalk featured also a small area of normal colonic mucosa (green rectangle, top). As previously shown (Chi et al., 1998), the bulk of these polyps lose the WT *PTEN* allele while retaining the mutant and thus are expressing only the $PTEN^{K289E}$ protein that we sought to study by immunohistochemistry. As depicted, the dysplastic surface area retains PTEN expression (consistent with loss of the WT *PTEN* copy and demonstrating $PTEN^{K289E}$ stability), yet magnification reveals that, surprisingly, PTEN is excluded from cell nuclei of epithelial cells (Figure 1D, right panel series). Remarkably, interstitial lymphocytes, which retain both WT and K289E mutant protein (Chi et al., 1998), in contrast also retain nuclear PTEN staining, serving as internal control for the staining procedure (right and left panel series, lowest panels, ly versus ep). Intriguingly, epithelial cells in the normal areas of the polyp's stalk, areas that typically retain both mutant and WT *PTEN* copies, display strong nuclear and cytoplasmic PTEN staining (left panel series), very similar to interstitial lymphocytes (high magnification, lowest panel). Identical results were obtained when using two different antibodies for staining (see Experimental Procedures). Thus, the K289E mutant protein appears to display an aberrant subcellular localization, reminiscent of a nuclear exclusion phenotype.

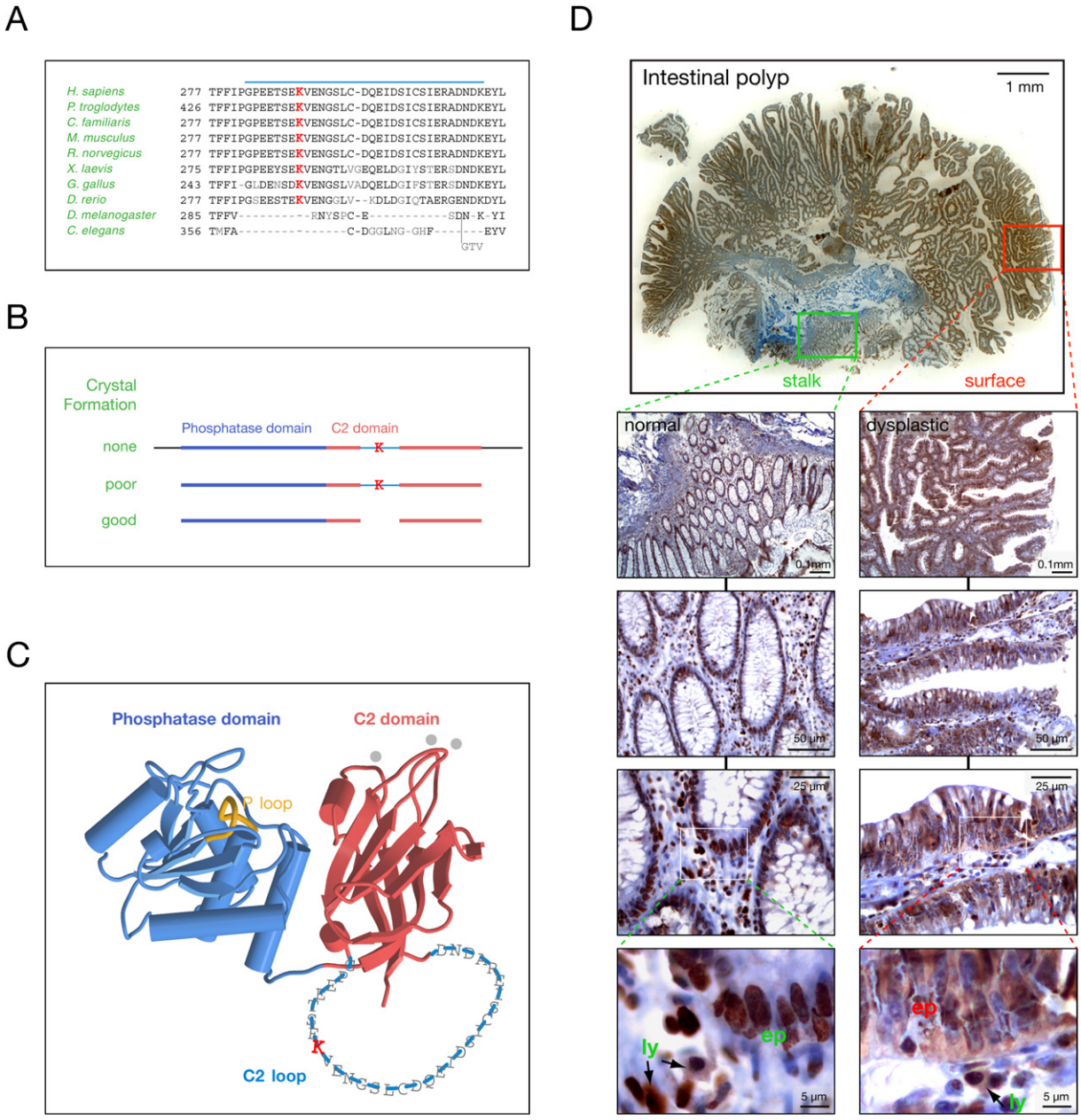

Figure 1. The PTEN^{K289E} Cowden Mutant Shows Nuclear Exclusion in Patient Samples

(A) Sequence alignment of the PTEN C2 loop (blue bar) from various species shows K289 conservation in vertebrates (highlighted in red).

(B) PTEN cleavage requirements for crystallization reveal that the C2 loop does not contribute to structural integrity (K denotes K289).

(C) Localization and size of the C2 loop within the PTEN structure (single amino acid code over backbone). Note that the C2 loop faces away from the cell membrane (top) and membrane-interacting loops of the C2 domain (gray dots).

(D) Intestinal polyp from a PTEN$^{wt/K289E}$ Cowden patient shows nuclear and cytoplasmic PTEN in normal (PTEN$^{wt/K289E}$) mucosa (left panel magnification series, green) and only cytoplasmic PTEN^{K289E} in dysplastic (PTEN$^{\Delta/K289E}$) regions (right panel magnification series, red). "ly" denotes circulating lymphocytes (PTEN$^{wt/K289E}$), and "ep" denotes epithelial cells.

Intrinsic Nuclear Import Defect of PTEN^{K289E}

Since the above-shown mislocalization could be either an intrinsic property of the K289E mutation or a polyp-specific effect on PTEN^{K289E}, we analyzed the mutants' subcellular distribution in vitro. By immunofluorescence (IF), endogenous PTEN is found in both cell nuclei and cytoplasm of most common human and murine cell lines and primary murine cells (data not shown), similar to the localization shown in the *PTEN* heterozygous prostate cancer cell line DU-145 (Figure 2A). To test mutant PTEN localization,

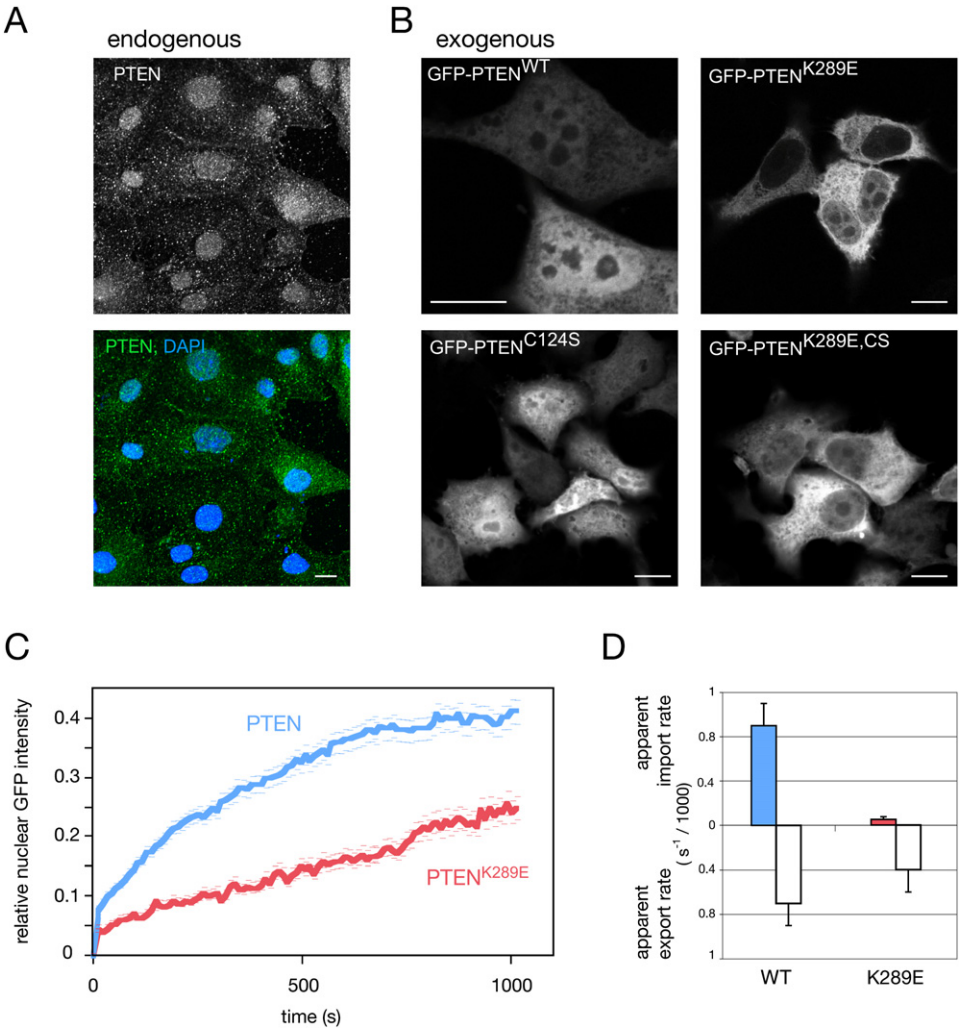

Figure 2. The PTEN^{K289E} Cowden Mutant Has an Intrinsic Nuclear Import Defect

(A) IF of endogenous PTEN in prostate cancer-derived *PTEN*$^{+/-}$ DU-145 cells. Scale bar, 10 μm.

(B) Localization of GFP-PTEN fusions reveals nuclear exclusion of the K289E mutant at 12 hr posttransfection. Scale bars, 10 μm.

(C) FRAP analysis of WT and PTEN^{K289E} shows nuclear accumulation after nuclear photobleaching. Error bars show standard deviation (SD).

(D) Quantification of (C) and quantification of nuclear export FRAP results for WT and mutant proteins. Error bars show SD.

PTEN-deficient prostate cancer cells (PC3) were transiently transfected. When overexpressed as GFP fusion, WT PTEN efficiently equilibrated between nucleus and cytoplasm within 10–12 hr after transfection (Figure 2B). Of note, PTEN localization was unaffected by catalytic activity, as revealed by the distribution of the enzyme-dead PTEN^{C124S} mutant (lower left panel), demonstrating that AKT activity (which is high in PC3 cells and only lowered upon WT PTEN transfection) does not visibly affect PTEN localization. Strikingly, at this time point the PTEN^{K289E} mutant showed dominant cytoplasmic accumulation in most cells, which is also unaffected by loss of enzymatic activity in the PTEN$^{K289E, C124S}$ double mutant (Figure 2B, right). The same results were obtained by visualizing non GFP-tagged PTEN and the corresponding mutants (Figure S1A, top). Notably, nuclear staining of the K289E mutant was found to increase by 24 and 48 hr after transfection (data not shown). Since steady-state cytoplasmic accumulation can in principle result from reduced nuclear import or enhanced nuclear export of PTEN^{K289E} (indicative of a loss- or gain-of-function mutation, respectively), we next tested the nuclear and cytoplasmic accumulation rates of the PTEN mutant quantitatively. The fluorescence recovery after photo bleaching (FRAP) technique produces distinguishable (yet chemically identical) cytoplasmic and nuclear PTEN populations by bleaching GFP fluorescence in either the cell nucleus or cytoplasm. Then the compartmental equilibration, which occurs via nuclear import and export, can be measured by time-lapse fluorescence microscopy (see Experimental Procedures).

We found that WT PTEN fluorescence reaccumulated inside the nucleus, reaching equilibrium by roughly 15

min post-nuclear bleaching (Figure 2C). The PTEN^{K289E} mutant, in contrast, showed clearly reduced nuclear accumulation and no equilibration within the same time. Calculation of the nuclear accumulation rates (i.e., apparent nuclear import rates) revealed an 18-fold reduction in nuclear net import for the K289E mutation (Figure 2D). Notably, dynamic analysis revealed that even when steady-state nuclear levels of WT and mutant PTEN appear to be similar (by static analysis), the mutant still shows a strongly reduced rate of nuclear accumulation. Importantly, the apparent export rate of the mutant protein was also decreased (Figure 2D), excluding a gain-of-export function through the K289E mutation. This result also excludes the possibility that WT nuclear localization is due to nuclear retention via K289 (which would result in higher K289E export rates). To exclude charge-conversion effects associated with the K289E mutation, the K289R mutant was measured and also revealed PTEN import deficiency (Figure S1B). Also of note, intranuclear and intracytoplasmic diffusion coefficients (as measured by FRAP) were not affected by the mutation (data not shown, see Experimental Procedures). Therefore, taken together, our experiments revealed that PTEN^{K289E} has a nuclear import/export defect and thus represents a loss-of-function mutant, defective in nucleocytoplasmic shuttling.

Lysine 289 Is a Major Site for PTEN Ubiquitination

Given its exposure and accessibility, we sought to determine whether lysine 289 (K289) represented a PTEN ubiquitination site. Ubiquitination is catalyzed by the sequential action of an E1 enzyme that transfers activated ubiquitin (Ub) to an E2 ligase. This, in concert with an E3 ligase, mediates ubiquitination of target proteins, usually on several variable target lysines, thus defining a system of utmost importance to cancer biology (Hershko and Ciechanover, 1998; Hoeller et al., 2006). We have identified NEDD4-1 as the major E3 Ub ligase of PTEN (Wang et al., 2007 [this issue of *Cell*]) and therefore tested whether NEDD4-1 ubiquitinates K289 in an in vitro assay. We used purified PTEN as a substrate and lysine-free Ub (KØ-Ub) to prevent poly-Ub chain formation and promote ubiquitination of all available sites on PTEN, visible as discrete bands in PTEN western blotting. As shown in Figure 3A (left lanes, WT), incubation of PTEN with the E2 ligase alone showed three specific adducts, likely representing single-, dual-, and triple-monoubiquitinated forms of PTEN, while addition of NEDD4-1 revealed at least seven discrete adduct forms of PTEN, consistent with the role of NEDD4-1 as E3 ligase. When carrying out this assay with the purified PTEN^{K289E} mutant, we found that at least one adduct band was missing, strongly suggesting that K289 is a target lysine for PTEN ubiquitination (Figure 3A, right lanes, K289E).

Since lack of ubiquitination in this system could also be due to an indirect effect of the mutation, we sought to confirm K289 ubiquitination directly by mass spectrometry (MS). However, our attempts at identifying even the unmodified tryptic fragment containing the K289 residue by MS failed because the tryptic loop fragment was too large to be retrieved in sample preparation (see Experimental Procedures). Therefore, we engineered two tryptic target sites flanking K289 into the C2 loop to produce PTEN^{RKR} (Figure 3B, top), which was indistinguishable from WT PTEN regarding enzymatic activity (see Figure S1C in the Supplemental Data available with this article online). GST-fused PTEN^{RKR} was ubiquitinated in vitro, enriched, and purified by GST pull-down, and, after SDS-PAGE/Coomassie staining, the fast migrating unmodified PTEN^{RKR} (below referred to as PTEN) and the first shifted band (termed +1) were both excised and processed for MS analysis. As intended, two expected tryptic fragments of the C2 loop (see Figure 3B, middle, fragments "I" and "II") were now clearly detectable by analysis of the PTEN band, demonstrating that the main PTEN Coomassie band contained only the unmodified C2 loop (Figure 3C, see upper panels for masses and lower panels for MS spectra). Analysis of the +1 band, in contrast, revealed a higher mass peptide of 1507.70 Da, as predicted for the loop peptide linked by branching to two additional glycine residues, the leftover of a Ub adduct after tryptic digestion (Figure 3C, PTEN-Ub, and Figure 3B, lowest panel). Thus, K289 is a target lysine for PTEN ubiquitination, coherent with its structural exposure in the C2 loop.

A Second, N-Terminal Ubiquitination Site Is Mutated in Cancer and Regulates PTEN Import

To test for the presence of Ub adducts on PTEN residues in cells, samples obtained from PTEN overexpression/immunoprecipitation (IP) in PC3 cells were processed for MS, which resulted in the identification of another Ub-adduct site, PTEN K13 (see Experimental Procedures). The molecular weight of the tryptic T peptide including K13 was measured at 956.579 Da (Figure 3D). Similar to the internal C2 loop, the N-terminal 13 residues of PTEN are also unstructured and exposed (Lee et al., 1999) and thus form targets for posttranslational modification. Strikingly, K13 of PTEN is also found mutated to glutamic acid (K13E) in spontaneous cancer (Duerr et al., 1998). To test whether this mutation also affects PTEN shuttling, we analyzed its localization. As shown in Figure 3E, PTEN^{K13E} was enriched in the cytoplasm and FRAP analysis revealed a defect in nuclear import as well as export (Figure 3F, data not shown). Notably, as shown in Figure S1D, K13 is also highly conserved.

Since K13 is part of a positively charged cluster (RNKRR), which could potentially function as an SV-40-type NLS for PTEN, the K13E mutation could simply be disrupting a basic NLS by replacing a positive charge with the negative charge of glutamic acid. We therefore tested whether the charge-conserving but ubiquitination-abolishing K13R mutation could still impeach import. Also, this mutant displayed strong cytoplasmic accumulation due to a nuclear import defect (Figures 3E and 3F, K13R), demonstrating that the positively charged patch does not function as PTEN-specific NLS but instead that the presence of the lysine residue is required, consistent with requirement for its ubiquitination to regulate import.

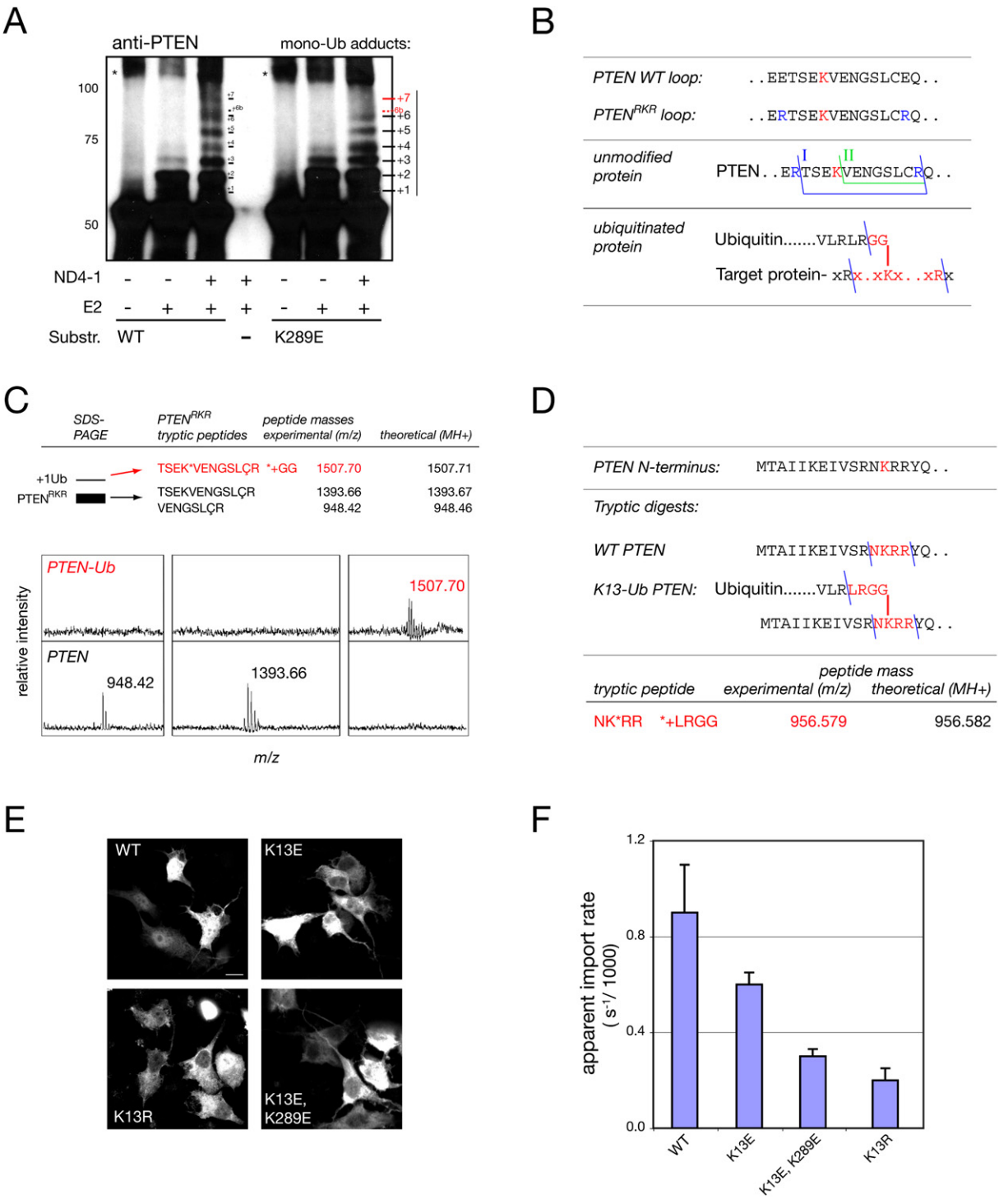

Figure 3. K13 and K289 Are Major Sites of PTEN Ubiquitination

(A) In vitro PTEN monoubiquitination assays using NEDD4-1 E3 ligase (ND4-1) reveal several target sites in WT PTEN and loss of at least one corresponding target site(s) ("+7/6b") in the K289E mutant (red). Note that numbering reflects only an estimate of the true adduct number. Asterisks denote non-Ub-specific aggregates. Molecular weights in kDa.

(B) (Top) Location of engineered tryptic sites for MS identification in PTEN^{RKR}. (Middle) The two expected tryptic C2 loop fragments for PTEN^{RKR} (I and II). (Bottom) Expected fragment for K289-ubiquitinated PTEN^{RKR} (red).

(C) MS of PTEN^{RKR} and the first adduct band reveals the expected fragments for unmodified PTEN and PTEN ubiquitinated at K289 (top, red). Lower panels show spectra of unmodified and modified PTEN with masses. "Ç" denotes cysteine-acryl-amide (see Experimental Procedures).

Our experiments with the K13E, K289E double mutant revealed that the two lysine residues can cooperate in promoting PTEN import (Figure 3F, K13E, K289), consistent with the notion that they are part of the limited set of Ub target lysines of PTEN (revealed in Figure 3A).

Taken together, we have identified two lysine residues that function as ubiquitination sites, are essential for PTEN shuttling and import, and are implicated in hereditary (K289E) and spontaneous (K13E) cancer.

PTEN Ubiquitination In Vivo

Next, we asked to what extent PTEN ubiquitination was occurring in vivo. While endogenous PTEN is efficiently mono- and polyubiquitinated upon overexpression of His-tagged Ub (Wang et al., 2007), overexpressed PTEN was found similarly ubiquitinated in cells: western blot analysis of lysates stained for PTEN revealed the appearance of two PTEN-specific slower migrating bands (Figure 4A) that increased over time (using two different antibodies, see Experimental Procedures). In addition, a smear was seen at later time points, as expected for polyubiquitination. The discrete bands comigrated with various tagged forms of PTEN, as expected for covalently linked adducts (Figure 4B, see also Figure S1E for lower exposure). To test whether these adducts were indeed formed by Ub, we coexpressed both KØ-Ub and WT Ub plasmids together with GFP-PTEN followed by IP. As shown, overexpression of PTEN and KØ-Ub resulted in several discrete mono-Ub adducts, bands that were even more prominent upon coexpression of unmodified Ub (Figure 4C, left, 1–3) due to the nature of that plasmid (see Experimental Procedures, Figure 5C, and Figure S1F for expression efficiencies and levels of the Ub plasmids). Ub overexpression also prompted a strong nonresolvable smear of polyubiquitinated PTEN (Figure 4C, left, poly). Analyzed vis-à-vis the PTEN input, the discrete bands coincided with the shifted bands of PTEN in a pattern similar to the one shown above but revealing an additional adduct (termed +1) (Figure 4C, right). Our results therefore showed that, similar to endogenous PTEN (Wang et al., 2007), overexpressed PTEN forms mono- as well as poly-Ub adducts in cells.

Next, we sought to determine whether the lysine mutants show a ubiquitination defect. To this end, we made use of a GFP-PTEN-KØ-Ub (GFP-PTEN-Ub-KØ) fusion protein (see Experimental Procedures). As shown in Figure 4D, this PTEN construct is present at lower levels in cells due to massive ubiquitination (for unknown reasons) resulting in its degradation, yet it does not appear to affect general ubiquitination (right). This tool allowed us to study PTEN ubiquitination directly by enhancing ubiquitination of PTEN exclusively, in contrast to Ub overexpression or proteasome inhibition, which enhances ubiquitination of all cellular Ub target proteins.

To test the contribution of K289 and K13 to PTEN ubiquitination, cells were transfected with the GFP-PTEN-Ub-KØ-K289E and GFP-PTEN-Ub-KØ-K13E mutants, respectively. As shown (Figure 4E), the WT fusion protein displayed a distinct mono-Ub band as well as a poly-Ub smear (note molecular weights), which characteristically extended into the stacking gel. Notably, the mono-Ub-specific shift (Figure 4E, mono-Ub) was clearly reduced in both the K13 and K289 mutants (see magnification and quantification in Figure 4E, right), confirming the function of these lysines as important targets for PTEN monoubiquitination in vivo. Note that forced Ub overexpression, in contrast, always rescued PTEN mutant ubiquitination, as expected given the number of possible target sites (data not shown, see also Figures 5C and 5D, below).

Monoubiquitination Dictates PTEN Nuclear Import

Ub has previously been linked to protein transport (Li et al., 2003; Lohrum et al., 2001; Massoumi et al., 2006; Plafker et al., 2004), and we sought to determine whether it could affect PTEN shuttling by FRAP. Ub coexpression resulted in a significant acceleration of PTEN nuclear import (Figure 5A, left). Quantification revealed a >50% increase in apparent import rates and export rates (Figure 5A, right), suggesting that PTEN ubiquitination may enhance shuttling. Moreover, we found that the nuclear resident fraction of PTEN was also increased upon Ub overexpression (Figure 5B, compare PTEN and PTEN + Ub in nuclear fractions). Notably, nuclear PTEN was not quantitatively monoubiquitinated, suggesting that PTEN is deubiquitinated to remain nuclear or else re-exported. In sum, our results demonstrated that ubiquitination positively affects PTEN shuttling, complementing the finding of reduced ubiquitination and transport of the PTEN mutants.

To test whether the nuclear import defect of the K289E mutant could be overcome by forced ubiquitination, we coexpressed PTEN^{K289E} with Ub and assessed PTEN localization by IF at 12 hr posttransfection. As shown in Figure 5C, PTEN^{K289E} was enriched in the cytoplasm while WT PTEN had equilibrated into the nucleus at this time point. Ub coexpression, in contrast, resulted in nuclear accumulation of the PTEN^{K289E} mutant (Figure 5C, K289E + Ub). Because the Ub plasmid promotes both PTEN mono- and poly-Ub formation (see Figure 4C), we next tested whether the KØ-Ub construct, which only supports monoubiquitination, was also able to rescue import. Indeed, cells cotransfected with the K289E mutant and KØ-Ub displayed very clear nuclear PTEN^{K289E} staining, strongly suggesting that mono-Ub suffices to rescue the import defect. To confirm and quantify these results, we performed rescue experiments using FRAP. Figure 5D shows that coexpression of PTEN^{K289E} and the Ub plasmid similarly enhanced the overall import of the mutant (Figure 5D, left, K289E + Ub). But most importantly,

(D) MS of immunoprecipitated PTEN after overexpression in cells reveals the peptide expected for a tryptic Ub adduct on K13.
(E) IF staining of GFP-tagged K13 mutants. Scale bar, 10 μm.
(F) FRAP and quantification of the apparent import rates of mutants visualized in (E). Error bars show SD.

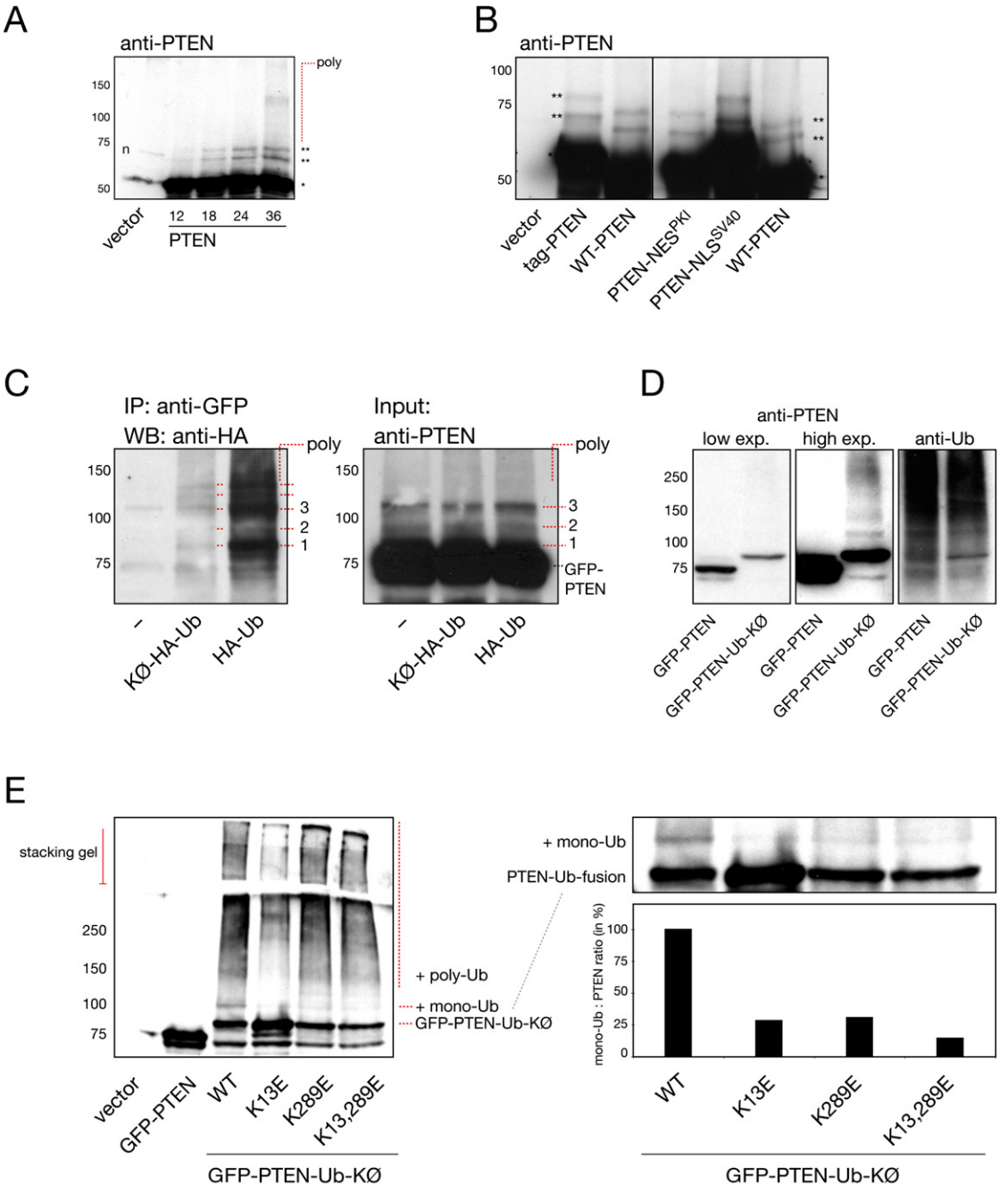

Figure 4. K13 and K289 Are Ubiquitinated In Vivo

(A) PTEN shows adduct formation in vivo and a smear (poly) at 36 hr posttransfection. Molecular weights in kDa. "n" denotes a nonspecific band, and asterisks indicate migration of unmodified (single) and modified (double) PTEN.

(B) Discrete adducts comigrate with various PTEN fusions. Asterisks as in (A). Molecular weights in kDa.

(C) Immunoprecipitation of GFP-PTEN after HA-Ub coexpression confirms discrete mono- (labeled 1–3) and poly-Ub adducts (labeled poly). Migration of GFP-PTEN is shown. Molecular weights in kDa.

(D) Low steady-state levels (left), strong ubiquitination (middle), and PTEN-specific ubiquitination (right) of the GFP-PTEN-Ub-KØ fusion. Molecular weights in kDa.

(E) Defects in monoubiquitination of the indicated lysine mutants. Left panel shows overview (location of stacking gel and molecular weights are indicated), and right panels show magnification and quantification of ratios for mono-Ub:main PTEN band intensities.

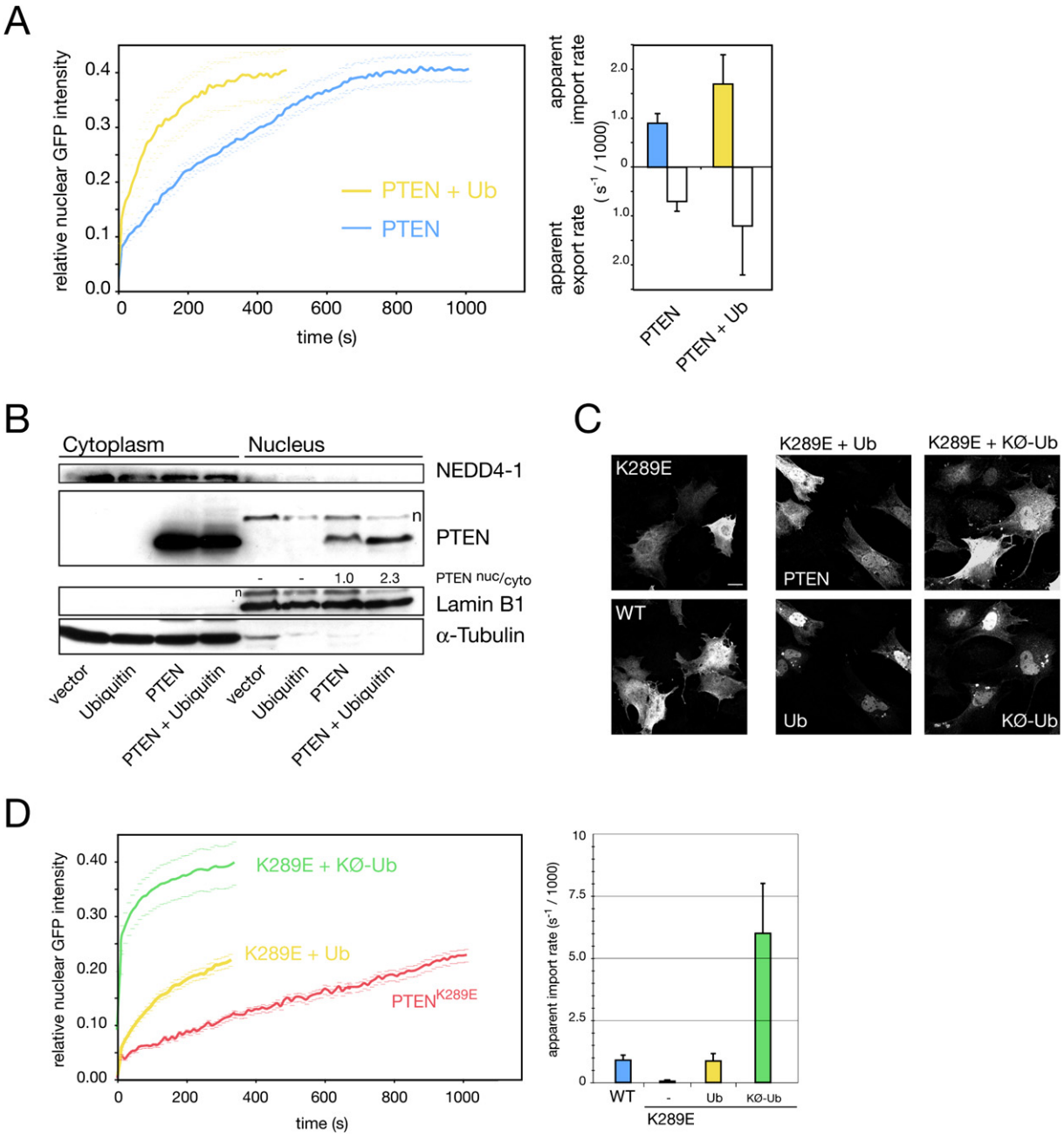

Figure 5. Monoubiquitination Regulates PTEN Nuclear Import and Shuttling

(A) FRAP assay measuring effect of Ub overexpression on PTEN import (left) and quantification of nuclear and cytoplasmic PTEN accumulation rates (right). Error bars show SD.

(B) Nuclear/cytoplasmic fractionation of PTEN after Ub overexpression. Lamin B1 and α-tubulin serve as nuclear and cytoplasmic markers, respectively. Numbers denote nuclear to cytoplasmic PTEN ratios (relative to lamin and tubulin, see Supplemental Data). A non-PTEN-specific band is indicated (n).

(C) IF imaging of PTEN and K289E with Ub coexpression. Scale bar, 10 μm.

(D) Ubiquitination rescues K289E nuclear import defect as measured by FRAP (left; quantifications, right). Note that monoubiquitination is most efficient in rescuing. Error bars show SD.

coexpression of the KØ-Ub mutant accelerated $PTEN^{K289E}$ import far more efficiently (K289E + KØ-Ub). Quantification of this rescue series showed that while Ub reset the K289E defect to approximately WT PTEN import levels, coexpression of KØ-Ub was 7-fold more powerful (right, K289E + KØ-Ub).

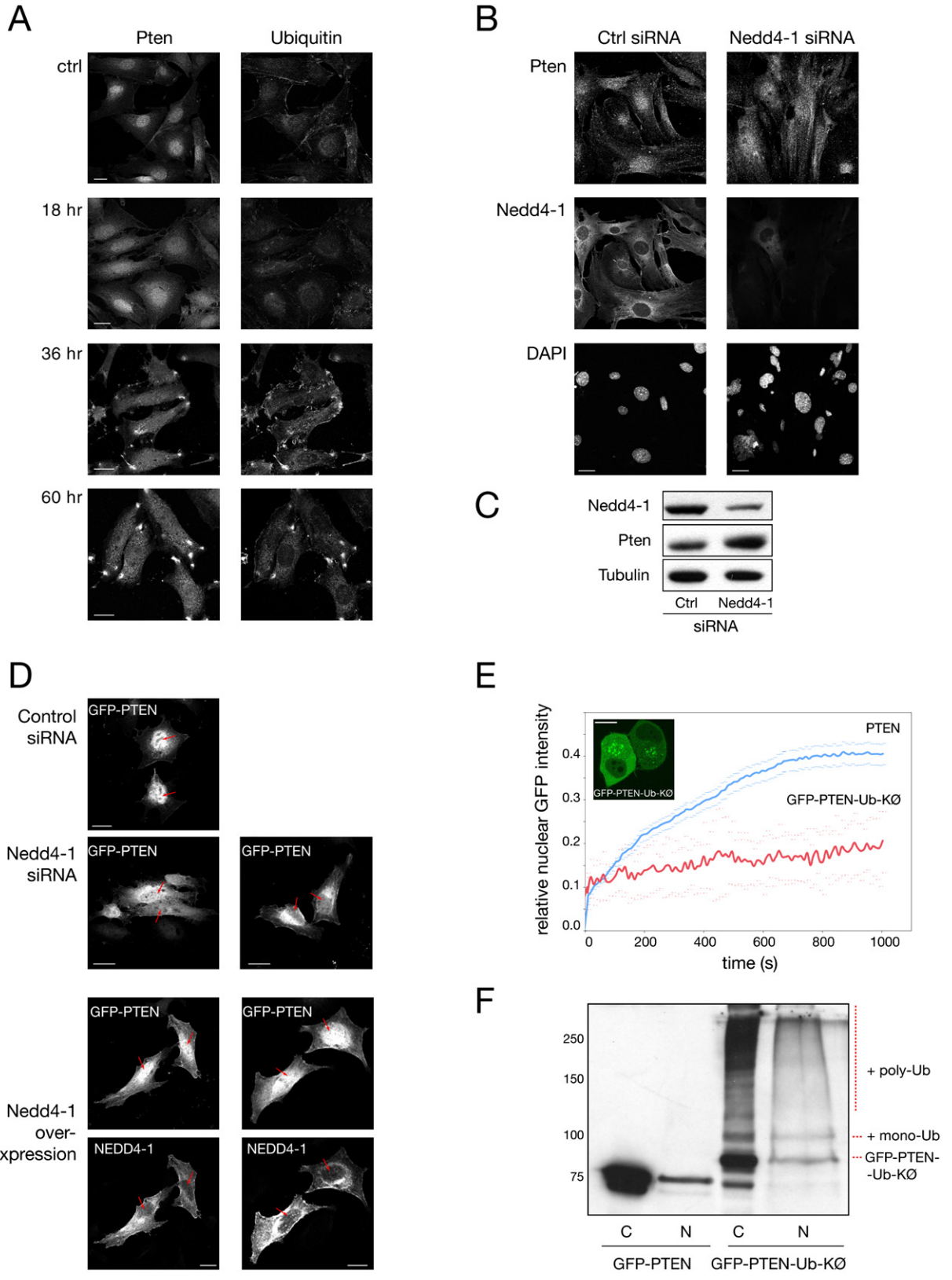
A
Pten
Ubiquitin
ctrl
18 hr
36 hr
60 hr
B
Ctrl siRNA
Nedd4-1 siRNA
Pten
Nedd4-1
DAPI
C
Nedd4-1
Pten
Tubulin
Ctrl
Nedd4-1
siRNA
D
Control siRNA
Nedd4-1 siRNA
Nedd4-1 over-expression
GFP-PTEN
NEDD4-1
E
relative nuclear GFP intensity
0.0
0.1
0.2
0.3
0.4
0
200
400
600
800
1000
time (s)
PTEN
GFP-PTEN-Ub-KØ
F
250
150
100
75
+ poly-Ub
+ mono-Ub
GFP-PTEN-Ub-KØ
C
N
C
N
GFP-PTEN
GFP-PTEN-Ub-KØ

Next, we sought to determine whether endogenous PTEN localization could be affected by lack of ubiquitination. To this end, we used the temperature-sensitive cell line *ts20*, in which ubiquitination is strongly reduced due to E1 ligase disruption at the restrictive temperature (Chowdary et al., 1994). As shown (Figure 6A), Pten localization at the permissive temperature was strongly nuclear in these NIH 3T3-derived cells, similar to the corrected control subline H35 before or after temperature shift and similar to endogenous Pten localization in mouse embryonic fibroblasts (MEFs, Figure 6B). But already 18 hr after the temperature shift, Pten started to accumulate in the cytoplasm, leading to a strong cytoplasmic stain by 36 and 60 hr, consistent with an import defect of newly synthesized Pten. As expected, the cells also revealed an aberrant Ub-localization pattern at 36 and 60 hr (Figure 6A, right).

To test whether the Ub-mediated PTEN transport was indeed due to direct ubiquitination of PTEN, we studied the role of the PTEN-targeting E3 ligase, NEDD4-1, in PTEN localization. Transient transfection of MEF cells with control siRNA showed dominant nuclear Pten and strong cytoplasmic Nedd4-1 localization (Figure 6B). Nedd4-1 knockdown, in contrast, led to a redistribution of Pten into the cytoplasm. Thus, we were able to phenocopy the effect of E1 ligase deficiency on PTEN localization by disruption of Nedd4-1. Importantly, Nedd4-1 mediated Pten import in addition to Pten degradation (see Figure 6C and Discussion). Similarly, knockdown of NEDD4-1 led to a cytoplasmic and perinuclear accumulation of exogenous PTEN in HeLa cells, while co-overexpression with GFP-PTEN resulted in strong nuclear PTEN (Figure 6D). Because NEDD4-1 in addition to PTEN polyubiquitination also mediates its monoubiquitination in vitro and in vivo (Wang et al., 2007), we conclude that PTEN monoubiquitination at discrete lysines, including K13 and K289, directly regulates its import and shuttling. Consequently, the small pool of discretely shifted monoubiquitinated PTEN shown in Figures 4A–4C represents the steady-state PTEN fraction that is shuttling competent.

Polyubiquitination, in contrast, resulted in cytoplasmic PTEN retention: the GFP-PTEN-Ub-KØ mutant, which was characterized by strong polyubiquitination in SDS-PAGE analysis (Figures 4D and 4E), showed import defects when assayed by FRAP and cytoplasmic accumulation in IF (Figure 6E). To determine nucleocytoplasmic distribution of the clearly visible ubiquitinated forms of this fusion, nuclear and cytoplasmic fractions of these cells were analyzed by western blotting. As expected (Figure 6F), polyubiquitinated PTEN adducts were exclusively cytoplasmic while the GFP-PTEN-Ub-KØ fusion itself displayed a distribution similar to GFP-PTEN. In contrast, the monoubiquitinated form, which largely depends on K13 and K289 availability (see Figure 4E), was specifically enriched in the nuclear fraction (10-fold compared to nonmodified PTEN, see quantification in Figure S1G), confirming that monoubiquitinated PTEN is shuttling most efficiently. Notably, these results also suggested that the pseudoubiquitination, which fuses Ub in frame to PTEN (GFP-PTEN-Ub-KØ), does not increase PTEN shuttling and thus cannot mimic the effect of ubiquitination on the true target sites.

Nuclear PTEN Is Stable, Active, and Rarely Found in Late-Stage Colon Cancer

We next sought to determine why loss of nuclear PTEN localization could be oncogenic. To this end, we first determined PTEN half-life after forced localization to the nuclear or cytoplasmic compartment using PTEN-NLS^{SV-40} or PTEN-NES^{PKI} (see Figure S1A, lowest panels). While WT PTEN, which as demonstrated above is both nuclear and cytoplasmic, showed a half-life of roughly 7.5 hr (Figure 7A), forced cytoplasmic accumulation led to a clear decrease in stability ($t^{1/2}$ = 4.5 hr), while nuclear localization resulted in increased stability ($t^{1/2}$ = 15 hr) as predicted because NEDD4-1 is mostly cytoplasmic (see Figures 5B, 6B, and 6D). To test nuclear PTEN activity, we next measured its ability to antagonize AKT. As shown (Figure 7B), transfection of increasing amounts of PTEN into PTEN-deficient PC3 cells resulted in 75% reduction (compared to the control) in the phospho-AKT:AKT ratio. But surprisingly, forced nuclear PTEN was still able to antagonize AKT activation, similar to forced cytoplasmic (unstable) PTEN.

Next, we tested whether nuclear PTEN was also able to induce apoptosis. After transfection of PC3 cells, cleaved caspase-3 staining was performed and positive cells were counted. PTEN-NES transfection into these p53-deficient cells resulted in an apoptotic index of 4.4 (±1.7) positive cells per 1000 (at 48 hr), while nuclear PTEN was as efficient with 4.8 positive cells (±1.3 per 1000), similar to PTEN transfection (3.1 ± 1.0 per 1000) and in contrast to vector transfection (0.4 ± 0.0 per 1000). In sum, our data showed that nuclear PTEN is more stable, can inhibit AKT, and is able to induce p53-independent apoptosis.

Finally, to test the general relevance of nuclear PTEN in the colon, we analyzed a tumor tissue microarray (TTM)

Figure 6. NEDD4-1 Dictates PTEN Localization in Murine and Human Cells

(A) Endogenous Pten shows an import defect in *ts20* cells after shift to the restrictive temperature for times indicated. Scale bars, 10 μm.

(B) Endogenous Pten shows cytoplasmic accumulation after knockdown of Nedd4-1 in MEF cells. Scale bars, 10 μm.

(C) Nedd4-1 siRNA efficiently reduces Nedd4-1 levels, resulting in a Pten increase in MEFs.

(D) NEDD4-1 siRNA and overexpression also dictate localization of overexpressed GFP-PTEN in HeLa cells. Arrows point at cell nuclei. Note perinuclear PTEN accumulation upon NEDD4-1 knockdown. Scale bars, 10 μm.

(E) FRAP measurement of GFP-PTEN-Ub fusion reveals import defect of polyubiquitinated PTEN and its dominant cytoplasmic localization by IF (insert). Error bars show SD. Scale bar, 10 μm.

(F) Fractionation and western analysis of GFP-PTEN and its fusion to Ub (GFP-PTEN-Ub-KØ). Note that the monoubiquitination band is the dominant form of PTEN that is specifically enriched in the nuclear fraction (+ mono-Ub).

A

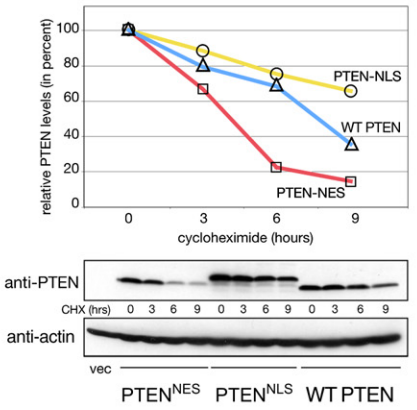

B

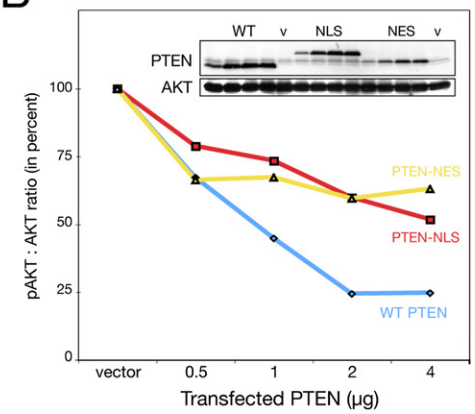

C

PTEN LOCALIZATION	TUMOR STAGE I-II	TUMOR STAGE III-IV
dominant nuclear	8 (73%)	3 (27%)
equally cytopl./nuclear	19 (35%)	35 (65%)
dominant cytoplasmic	12 (54%)	10 (46%)
total cases	39	48

p = 0.042

D

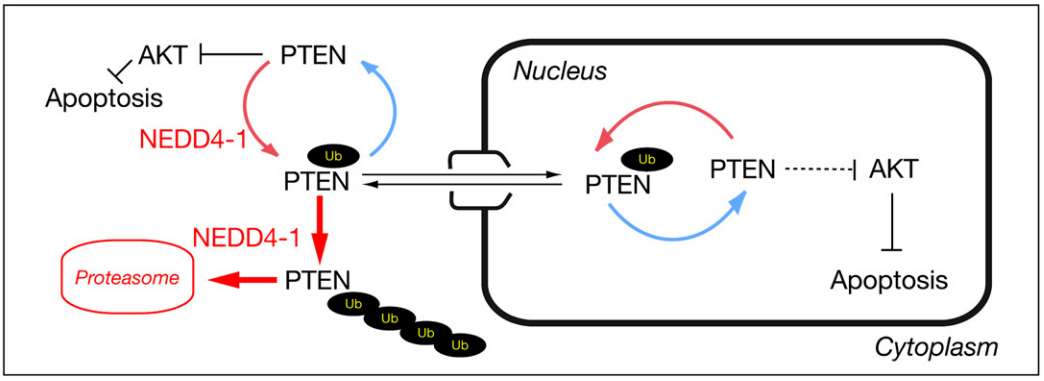

Figure 7. Nuclear PTEN Is Stable and Active In Vivo and Reduced in Late-Stage Colon Carcinoma

(A) Half-life of PTEN after forced nuclear (-NLS) or cytoplasmic (-NES) overexpression compared to WT PTEN in presence of cycloheximide (CHX). Densitometry quantification (PTEN: actin, upper panels) and raw data (lower panels) are shown. Control transfection is indicated (vec).

(B) Titration of nuclear versus cytoplasmic PTEN activity. Quantification of pAKT:AKT ratio and PTEN expression levels (inserts). "v" indicates vector control transfection. PTEN levels are shown, and AKT is used as loading reference.

(C) PTEN localization in TTM with specimens of 87 colon cancer patients reveals positive correlation between nuclear PTEN localization and low tumor grade. Statistical significance is indicated (p, see also Experimental Procedures).

with specimens of 87 colon cancer patients for tumor grade and PTEN localization (PTEN-negative samples were significantly associated with advanced tumor stage, $p < 0.022$, and were omitted for this analysis). As summarized in Figure 7C, we found that samples with high nuclear PTEN staining significantly associated with less advanced pathological stage. In addition, an increase in even nucleocytoplasmic PTEN distribution was associated with higher tumor stage, consistent with previous findings (Zhou et al., 2002). Taken together, these data were in agreement with the notion that tumors that can retain a strong nuclear PTEN staining remain of lower grade.

DISCUSSION

The molecular makeup of spontaneous cancers at the clinical stage usually presents a complex mixture of primary and consequential events, some of which are thought to contribute to essential aspects of tumor progression (Hanahan and Weinberg, 2000). Cancer syndrome-associated mutations, in contrast, often constitute well-defined primary tumorigenic events that are causal to tumor formation (Nagy et al., 2004). Specifically, germline mutation of *PTEN* has been shown to underlie the closely related autosomal dominant tumor susceptibility syndromes Cowden disease and Bannayan-Riley-Ruvalcaba syndrome (Eng, 2003). Therefore, we anticipated that *PTEN* germline mutations would hold valuable information and novel insights into PTEN function in tumor initiation. While most of the described mutations result in truncation, many PTEN missense mutations affect its catalytic activity. Through investigating instead how the enzymatically functional $PTEN^{K289E}$ mutant could be at the root of inheritable cancer, we have come to several novel conclusions:

(1) We have discovered that deficiency in PTEN import causes cancer susceptibility, independent of catalytic activity. While it has been previously shown that the $PTEN^{K289E}$ mutant retains catalytic activity (Georgescu et al., 2000), its nuclear import defect has so far remained elusive. Correlation of the K289E import defect with the observed cytoplasmic accumulation in the relevant Cowden patient tissue thus represents to our knowledge the first example of a causal relation between PTEN localization and cancer initiation. Since no such certainty on the cause-and-effect relation exists in sporadic mutations like $PTEN^{K13E}$ (which, as published, also suffers reduction in catalytic activity [Walker et al., 2004]), the K289E mutation allows us to unambiguously ascribe a tumor-suppressive function to PTEN nuclear localization. In agreement with this finding, we find significant correlation between low tumor stage in colon cancer and dominant nuclear PTEN localization.

(2) We show that nuclear PTEN import is regulated by monoubiquitination, which to our knowledge represents the first example of target protein ubiquitination enhancing nuclear import (and shuttling). PTEN polyubiquitination, in contrast, leads to its cytoplasmic retention and degradation (Ciechanover, 2005) and is therefore oncogenic in nature (see also Wang et al. [2007]). Thus, PTEN monoubiquitination and subsequent nuclear import has a protective function, a highly relevant finding for the discussion of NEDD4-1 in tumorigenesis (see below). As mentioned, Ub charging of some E2 ligases has been shown to regulate their nuclear import (Plafker et al., 2004), and, intriguingly, deubiquitination of the Bcl-3 transcription factor has been recently shown to cause its cytoplasmic accumulation (Massoumi et al., 2006). Yet Bcl-3 cytoplasmic accumulation due to loss of nuclear (Ub-mediated) retention cannot be excluded, in contrast to PTEN, where ubiquitination dictates the actual transport rates.
Monoubiquitination has previously been implied in p53 nuclear export (Li et al., 2003; Lohrum et al., 2001), but p53 also contains several well-characterized NLS and NES sequences that enhance transport (Michael and Oren, 2003). PTEN, in contrast, may rely entirely on the ubiquitination system for shuttling, since no transferable NLS-like sequences have been demonstrated for it and we have shown that the K13 cluster does not rely on charge for import. It will be interesting to see whether PTEN shares ubiquitination-specific import receptors with the above-mentioned cargoes.

(3) We identify K13 and K289 as two major and conserved sites for PTEN ubiquitination, and we show that their mutation leads to a constitutive shuttling defect that can be overcome by forced monoubiquitination. Importantly, PIP_2 phospholipid binding and allosteric PTEN activation functions have also been ascribed to the basic patch containing K13 (for a review see Leslie and Downes [2004]), and it will be interesting to see how these functions affect ubiquitination and vice versa.
Since further sites on PTEN can also be ubiquitinated both in vitro and in vivo, we hypothesize that monoubiquitination efficiency is a limiting step of PTEN shuttling, and that Ub proteases reverse this process and antagonize shuttling because the nuclear pool of PTEN is not quantitatively monoubiquitinated. Taken together, our data suggest a model (Figure 7D) in which cytoplasmic monoubiquitination of PTEN leads to either PTEN

(D) Model for regulation of PTEN import and shuttling versus PTEN degradation. PTEN is ubiquitinated in the cytoplasm by NEDD4-1, which allows for PTEN import. Alternatively, PTEN is ubiquitinated further in the cytoplasm and degraded by the proteasome. Nuclear PTEN can shuttle back to the cytoplasm or, after deubiquitination, remain nuclear and protected from cytoplasmic degradation. Importantly, nuclear PTEN is not only protected but is still able to antagonize AKT and cause apoptosis. Thus, PTEN-specific Ub ligases and proteases regulate PTEN localization, function, and stability.

import or, alternatively, polyubiquitination and PTEN degradation (by NEDD4-1). Nuclear PTEN-Ub can shuttle back to the cytoplasm or, after deubiquitination, remain nuclear and protected from cytoplasmic degradation until it is again monoubiquitinated and exported.

(4) We demonstrate that PTEN nuclear localization is coupled to activity of the only known PTEN E3 ligase, NEDD4-1, which can both mono- and polyubiquitinate PTEN in vitro and in vivo. Because we here show that monoubiquitination is essential for PTEN function, NEDD4-1 effectively has both oncogenic (PTEN degradation) and tumor-suppressive (PTEN shuttling) potential. Several scenarios of how PTEN levels and localization are regulated can therefore be envisioned: first, NEDD4-1 modification/protein association could switch it from mono- to polyubiquitination mode; second, NEDD4-1 localization could dictate PTEN levels in a particular compartment (in polyubiquitination mode) and/or transport out of the compartment (in monoubiquitination mode). In this respect, it is interesting to note that although many cells show dominant cytoplasmic NEDD4-1, some cell lines and certain murine tissues show strong nuclear NEDD4-1 (L.C.T. and P.P.P., unpublished data). Significantly, the above implications for NEDD4-1 localization and activity apply equally to PTEN deubiquitinases, which we propose to be essential for control of PTEN residence times and stability within the nuclear and cytoplasmic compartments as depicted (Figure 7D).

(5) We find that nuclear PTEN is not only protected but is still able to antagonize AKT and cause apoptosis. These findings are in line with our observation of dominant nuclear PTEN localization in early-stage, but not advanced-stage, colon cancer. Together with our observations in the Cowden patient tissue, these data suggest that retention of the nuclear import capability of PTEN is a critical tumor-suppressive determinant, and it will be interesting to see whether other patient-derived PTEN mutations also target PTEN import instead of catalytic activity. Taken together, we have, through an integrative approach, linked the genetics of a cancer syndrome with the biochemistry and cell biology of protein modification to demonstrate how ubiquitination regulates nuclear import and tumor progression through PTEN. We therefore propose that Ub is a decisive regulator of this major tumor suppressor and that further defining this process is crucial to understanding and developing ubiquitination-related cancer therapies.

EXPERIMENTAL PROCEDURES

Plasmids and Protein Purification

PTEN cloned into pcDNA3.1 (Lee et al., 1999) was subcloned into pEGFP-C2 and its derivatives constructed as described in the Supplemental Data section. The WT Ub plasmid contains eight tandems of HA-Ub under the CMV promotor. For protein production, PTEN, PTEN^{K289E}, and PTEN^{RKR} were expressed via baculovirus as detailed in the Supplemental Data.

In Vitro Ubiquitination Assays

Monoubiquitination reactions of WT PTEN and K289E mutant were carried out at 30°C for 2 hr in 40 mM Tris-HCl (pH 7.5), 2 mM DTT, and 5 mM $MgCl_2$, using 10 μg of KØ-Ub mutant (Boston Biochem, catalog number UM-NOK), 40 nM human E1 (Boston Biochem, catalog number E302), 8 μM UbCH5c, 5 mM ATP (Sigma, catalog number A-7699), 300 ng of recombinant PTEN or GST-PTEN-RKR, and 2 μl purified NEDD4-1 (see Wang et al. [2007]). See Supplemental Data for detailed information.

Cells, Western Blotting, and Immunocytochemistry

For IF, cells were prepared using standard preparation and confocal analysis procedures detailed in Supplemental Data. The *ts20* cell line was a kind gift from Dr. H. Ozer (New Jersey Medical School). Nedd4-1 knockdown was performed in *Trp53*$^{-/-}$ MEFs using the pSuper-Retra-LacZ (LacZi) or pSuper-Retra-Nedd4-1 (iN4A) plasmids (see Wang et al. [2007] and Supplemental Data). For protein half-life, cells were treated with 30 μg/ml cycloheximide as previously described (Chen et al., 2005). Half-life extrapolation, nucleocytoplasmic fractionation, apoptosis assays, and IPs were carried out using the standard methods described in the Supplemental Data section.

Photobleaching In Vivo Import/Export Assays

PC3 cells were plated, transfected with Lipofectamine 2000, and observed in LabTekII chambers (Nalgene) at 24 hr posttransfection (identical results were obtained at 36 hr, data not shown). Import/export assays were performed on a Zeiss LSM 510 confocal microscope and evaluated as described (see references and detailed methods in Supplemental Data).

Mass Spectrometry

Gel-resolved proteins "PTEN RKR" (control) and "Ub-PTEN RKR" derived from the ubiquitination reactions were digested with trypsin and batch purified on a reversed-phase microtip, and resulting peptide pools were individually analyzed by matrix-assisted laser desorption/ionization reflectron time-of-flight (MALDI-reTOF) MS (UltraFlex TOF/TOF; Bruker; Bremen, Germany) for peptide mass fingerprinting as described in Supplemental Data.

Immunohistochemistry on Patient Samples and Tumor Tissue Microarrays

Cowden patient colon sample slides were stained for PTEN using the monoclonal 6H2.1 (Cascade, Figure 1D) and polyclonal Ab-2 (Neomarkers) as previously described (Trotman et al., 2003). Tissue microarray construction, its staining, and scoring methods are detailed in Supplemental Data.

Statistical Analysis, Sequence Alignments, and PTEN Modeling

Statistical significance calculations, PTEN sequence alignments, and modeling are described in the Supplemental Data section.

Supplemental Data

Supplemental Data include one figure, Supplemental Experimental Procedures, and Supplemental References and can be found with this article online at http://www.cell.com/cgi/content/full/128/1/141/DC1/.

ACKNOWLEDGMENTS

We would like to thank Q. Li, S. Mabon, and M.S. Jiao for help with insect cell culture, FRAP, and pathology analysis, respectively. We would like to thank P. Bonner for data management, L. Lopez and

E. Iskidarova for technical assistance in tissue microarray construction, I. Linkov and M. Asher and the Pathology Core Laboratory at MSKCC for help with their expertise in IHC, and A. Nazarian for help with MS. This research was supported by the NIH grant R01-CA-82328 to P.P.P. and the NCI Cancer Center Support Grant P30-CA-08748 to P.T. and in part by the Intramural Research Program of the NIH, National Cancer Institute, Center for Cancer Research.

Received: March 9, 2006
Revised: July 2, 2006
Accepted: November 1, 2006
Published: January 11, 2007

REFERENCES

Bonneau, D., and Longy, M. (2000). Mutations of the human PTEN gene. Hum. Mutat. *16*, 109–122.

Cantley, L.C. (2002). The phosphoinositide 3-kinase pathway. Science *296*, 1655–1657.

Chen, Z., Trotman, L.C., Shaffer, D., Lin, H.K., Dotan, Z.A., Niki, M., Koutcher, J.A., Scher, H.I., Ludwig, T., Gerald, W., et al. (2005). Crucial role of p53-dependent cellular senescence in suppression of Pten-deficient tumorigenesis. Nature *436*, 725–730.

Chi, S.G., Kim, H.J., Park, B.J., Min, H.J., Park, J.H., Kim, Y.W., Dong, S.H., Kim, B.H., Lee, J.I., Chang, Y.W., et al. (1998). Mutational abrogation of the PTEN/MMAC1 gene in gastrointestinal polyps in patients with Cowden disease. Gastroenterology *115*, 1084–1089.

Chook, Y.M., and Blobel, G. (2001). Karyopherins and nuclear import. Curr. Opin. Struct. Biol. *11*, 703–715.

Chowdary, D.R., Dermody, J.J., Jha, K.K., and Ozer, H.L. (1994). Accumulation of p53 in a mutant cell line defective in the ubiquitin pathway. Mol. Cell. Biol. *14*, 1997–2003.

Ciechanover, A. (2005). Proteolysis: from the lysosome to ubiquitin and the proteasome. Nat. Rev. Mol. Cell Biol. *6*, 79–87.

Di Cristofano, A., and Pandolfi, P.P. (2000). The multiple roles of PTEN in tumor suppression. Cell *100*, 387–390.

Di Cristofano, A., Pesce, B., Cordon-Cardo, C., and Pandolfi, P.P. (1998). Pten is essential for embryonic development and tumour suppression. Nat. Genet. *19*, 348–355.

Di Cristofano, A., De Acetis, M., Koff, A., Cordon-Cardo, C., and Pandolfi, P.P. (2001). Pten and p27KIP1 cooperate in prostate cancer tumor suppression in the mouse. Nat. Genet. *27*, 222–224.

Duerr, E.M., Rollbrocker, B., Hayashi, Y., Peters, N., Meyer-Puttlitz, B., Louis, D.N., Schramm, J., Wiestler, O.D., Parsons, R., Eng, C., and von Deimling, A. (1998). PTEN mutations in gliomas and glioneuronal tumors. Oncogene *16*, 2259–2264.

Eng, C. (2003). PTEN: one gene, many syndromes. Hum. Mutat. *22*, 183–198.

Georgescu, M.M., Kirsch, K.H., Kaloudis, P., Yang, H., Pavletich, N.P., and Hanafusa, H. (2000). Stabilization and productive positioning roles of the C2 domain of PTEN tumor suppressor. Cancer Res. *60*, 7033–7038.

Gorlich, D., and Kutay, U. (1999). Transport between the cell nucleus and the cytoplasm. Annu. Rev. Cell Dev. Biol. *15*, 607–660.

Hanahan, D., and Weinberg, R.A. (2000). The hallmarks of cancer. Cell *100*, 57–70.

Hershko, A., and Ciechanover, A. (1998). The ubiquitin system. Annu. Rev. Biochem. *67*, 425–479.

Hoeller, D., Hecker, C.M., and Dikic, I. (2006). Ubiquitin and ubiquitin-like proteins in cancer pathogenesis. Nat. Rev. Cancer *6*, 776–788.

Lee, J.O., Yang, H., Georgescu, M.M., Di Cristofano, A., Maehama, T., Shi, Y., Dixon, J.E., Pandolfi, P., and Pavletich, N.P. (1999). Crystal structure of the PTEN tumor suppressor: implications for its phosphoinositide phosphatase activity and membrane association. Cell *99*, 323–334.

Leslie, N.R., and Downes, C.P. (2004). PTEN function: how normal cells control it and tumour cells lose it. Biochem. J. *382*, 1–11.

Li, J., Yen, C., Liaw, D., Podsypanina, K., Bose, S., Wang, S.I., Puc, J., Miliaresis, C., Rodgers, L., McCombie, R., et al. (1997). PTEN, a putative protein tyrosine phosphatase gene mutated in human brain, breast, and prostate cancer. Science *275*, 1943–1947.

Li, M., Brooks, C.L., Wu-Baer, F., Chen, D., Baer, R., and Gu, W. (2003). Mono- versus polyubiquitination: differential control of p53 fate by Mdm2. Science *302*, 1972–1975.

Lian, Z., and Di Cristofano, A. (2005). Class reunion: PTEN joins the nuclear crew. Oncogene *24*, 7394–7400.

Lohrum, M.A., Woods, D.B., Ludwig, R.L., Balint, E., and Vousden, K.H. (2001). C-terminal ubiquitination of p53 contributes to nuclear export. Mol. Cell. Biol. *21*, 8521–8532.

Ma, L., Teruya-Feldstein, J., Behrendt, N., Chen, Z., Noda, T., Hino, O., Cordon-Cardo, C., and Pandolfi, P.P. (2005). Genetic analysis of Pten and Tsc2 functional interactions in the mouse reveals asymmetrical haploinsufficiency in tumor suppression. Genes Dev. *19*, 1779–1786.

Maehama, T., and Dixon, J.E. (1998). The tumor suppressor, PTEN/MMAC1, dephosphorylates the lipid second messenger, phosphatidylinositol 3,4,5-trisphosphate. J. Biol. Chem. *273*, 13375–13378.

Massoumi, R., Chmielarska, K., Hennecke, K., Pfeifer, A., and Fassler, R. (2006). Cyld inhibits tumor cell proliferation by blocking Bcl-3-dependent NF-kappaB signaling. Cell *125*, 665–677.

Michael, D., and Oren, M. (2003). The p53-Mdm2 module and the ubiquitin system. Semin. Cancer Biol. *13*, 49–58.

Nagy, R., Sweet, K., and Eng, C. (2004). Highly penetrant hereditary cancer syndromes. Oncogene *23*, 6445–6470.

Nelen, M.R., van Staveren, W.C., Peeters, E.A., Hassel, M.B., Gorlin, R.J., Hamm, H., Lindboe, C.F., Fryns, J.P., Sijmons, R.H., Woods, D.G., et al. (1997). Germline mutations in the PTEN/MMAC1 gene in patients with Cowden disease. Hum. Mol. Genet. *6*, 1383–1387.

Plafker, S.M., Plafker, K.S., Weissman, A.M., and Macara, I.G. (2004). Ubiquitin charging of human class III ubiquitin-conjugating enzymes triggers their nuclear import. J. Cell Biol. *167*, 649–659.

Podsypanina, K., Ellenson, L.H., Nemes, A., Gu, J., Tamura, M., Yamada, K.M., Cordon-Cardo, C., Catoretti, G., Fisher, P.E., and Parsons, R. (1999). Mutation of Pten/Mmac1 in mice causes neoplasia in multiple organ systems. Proc. Natl. Acad. Sci. USA *96*, 1563–1568.

Sansal, I., and Sellers, W.R. (2004). The biology and clinical relevance of the PTEN tumor suppressor pathway. J. Clin. Oncol. *22*, 2954–2963.

Sherr, C.J. (2004). Principles of tumor suppression. Cell *116*, 235–246.

Stambolic, V., Suzuki, A., de la Pompa, J.L., Brothers, G.M., Mirtsos, C., Sasaki, T., Ruland, J., Penninger, J.M., Siderovski, D.P., and Mak, T.W. (1998). Negative regulation of PKB/Akt-dependent cell survival by the tumor suppressor PTEN. Cell *95*, 29–39.

Steck, P.A., Pershouse, M.A., Jasser, S.A., Yung, W.K., Lin, H., Ligon, A.H., Langford, L.A., Baumgard, M.L., Hattier, T., Davis, T., et al. (1997). Identification of a candidate tumour suppressor gene, MMAC1, at chromosome 10q23.3 that is mutated in multiple advanced cancers. Nat. Genet. *15*, 356–362.

Suzuki, A., de la Pompa, J.L., Stambolic, V., Elia, A.J., Sasaki, T., del Barco Barrantes, I., Ho, A., Wakeham, A., Itie, A., Khoo, W., et al. (1998). High cancer susceptibility and embryonic lethality associated with mutation of the PTEN tumor suppressor gene in mice. Curr. Biol. *8*, 1169–1178.

Trotman, L.C., and Pandolfi, P.P. (2003). PTEN and p53: who will get the upper hand? Cancer Cell *3*, 97–99.

Trotman, L.C., Niki, M., Dotan, Z.A., Koutcher, J.A., Cristofano, A.D., Xiao, A., Khoo, A.S., Roy-Burman, P., Greenberg, N.M., Dyke, T.V., et al. (2003). Pten dose dictates cancer progression in the prostate. PLoS Biol. *1*, E59. Published online October 27, 2003. 10.1371/journal.pbio.0000059.

Trotman, L.C., Alimonti, A., Scaglioni, P.P., Koutcher, J.A., Cordon-Cardo, C., and Pandolfi, P.P. (2006). Identification of a tumour suppressor network opposing nuclear Akt function. Nature *441*, 523–527.

Walker, S.M., Leslie, N.R., Perera, N.M., Batty, I.H., and Downes, C.P. (2004). The tumour-suppressor function of PTEN requires an N-terminal lipid-binding motif. Biochem. J. *379*, 301–307.

Wang, X., Trotman, L.C., Koppie, T., Alimonti, A., Chen, Z., Gao, Z., Wang, J., Erdjument-Bromage, H., Tempst, P., Cordon-Cardo, C., Pandolfi, P.P., and Jiang, X. (2007). NEDD4-1 is a proto-oncogenic ubiquitin ligase for PTEN. Cell *128*, this issue, 129–139.

Whiteman, D.C., Zhou, X.P., Cummings, M.C., Pavey, S., Hayward, N.K., and Eng, C. (2002). Nuclear PTEN expression and clinicopathologic features in a population-based series of primary cutaneous melanoma. Int. J. Cancer *99*, 63–67.

Zhou, X.P., Loukola, A., Salovaara, R., Nystrom-Lahti, M., Peltomaki, P., de la Chapelle, A., Aaltonen, L.A., and Eng, C. (2002). PTEN mutational spectra, expression levels, and subcellular localization in microsatellite stable and unstable colorectal cancers. Am. J. Pathol. *161*, 439–447.